EXPERIMENTAL and MOLECULAR MEDICINE, Vol. 40, No. 3, 304-312, June 2008
DOI 10.3858/emm.2008.40.3.304

Distal hereditary motor neuropathy in Korean patients with a small heat shock protein 27 mutation

Ki Wha Chung[1]*, Sang-Beom Kim[2]*, Sun Young Cho[3], Su Jin Hwang[3], Sun Wha Park[1], Sung Hee Kang[1], Joonki Kim[1], Jeong Hyun Yoo[4] and Byung-Ok Choi[3,5]

[1]Department of Biological Science
Kongju National University
Gongju 314-701, Korea
[2]Department of Neurology
Kyung Hee University
East-West Neo Medical Center
Seoul 134-727, Korea
[3]Department of Neurology
[4]Department of Radiology
Ewha Medical Research Center
Ewha Womans University, School of Medicine
Seoul 158-710, Korea
[5]Corresponding author: Tel, 82-2-2650-2842;
Fax, 82-2-2650-2652; E-mail, bochoi@ewha.ac.kr
*These authors contributed equally to this work.

Accepted 7 March 2008

Abbreviations: CMT, Charcot-Marie-Tooth disease; dHMN, distal hereditary motor neuropathy; FDS, functional disability scale; HSP27, heat shock protein 27; MRI, magnetic resonance imaging; NCV, nerve conduction velocity

Abstract

Distal hereditary motor neuropathy (dHMN) is a heterogeneous disorder characterized by degeneration of motor nerves in the absence of sensory abnormalities. Recently, mutations in the small *heat shock protein 27 (HSP27)* gene were found to cause dHMN type II or Charcot-Marie-Tooth disease type 2F (CMT2F). The authors studied 151 Korean axonal CMT or dHMN families, and found a large Korean dHMN type II family with the Ser135Phe mutation in *HSP27*. This mutation was inherited in an autosomal dominant manner, and was well associated with familial members with the dHMN phenotype. This mutation site is located in the α-crystallin domain and is highly conserved between different species. The frequency of this *HSP27* mutation in Koreans was 0.6%. Magnetic resonance imaging analysis revealed that fatty infiltrations tended to progressively extend distal to proximal muscles in lower extremities. In addition, fatty infiltrations in thigh muscles progressed to affect posterior and anterior compartments but to lesser extents in medial compartment, which differs from CMT1A patients presenting with severe involvements of posterior and medial compartments but less involvement of anterior compartment. The authors describe the clinical and neuroimaging findings of the first Korean dHMN patients with the *HSP27* Ser135Phe mutation. To our knowledge, this is the first report of the neuroimaging findings of dHMN type II.

Keywords: Asian continental ancestry group; Charcot-Marie-Tooth disease; heat-shock proteins; magnetic resonance imaging; spinal muscular atrophies of childhood

Introduction

Distal hereditary motor neuropathies (dHMNs) are pure motor peripheral neuropathies, but are otherwise a clinically and genetically heterogeneous group of disorders characterized by weakness and wasting of the distal muscles of both upper and lower limbs (Irobi *et al*., 2006). Distal HMN closely resembles Charcot-Marie-Tooth disease type 2 (CMT2), apart from the absence of the sensory abnormalities, and is difficult to distinguish from CMT2, because sensory signs are often lacking in CMT2 patients (Evgrafov *et al*., 2004; Tang *et al*., 2005). Therefore, clinical and electrophysiological examinations are essential to confirm a diagnosis of dHMN, or CMT2.

Mutations in the gene encoding the 27 kDa small heat shock protein 27 (HSP27, also called heat shock 27-kD protein 1, HSPB1) have been shown to be causal in Charcot-Marie-Tooth disease type 2F (CMT2F; OMIM 606595) and dHMN type II (OMIM 608634). Since mutations of the *HSP27* gene were first identified in an English family with dHMN type II and in Russian family with CMT2F in 2004, six missense mutations (Arg127Trp, Arg136Trp, Ser135Phe, Thr151Ile, Pro182Ser and Pro182Leu) have been discovered in families with dHMN or CMT2F (Evgrafov *et al*., 2004; Kijima *et al*., 2005; Tang *et al*., 2005). The

majority of *HSP27* mutations have been found in dHMN patients in the α-crystallin domain, excepting Pro182Ser and Pro182Leu, which are in the C-terminal extension (Evgrafov *et al*., 2004; Kijima *et al*., 2005). The α-crystallin domain is a highly conserved region within the small HSP superfamily and mutations in this motif can cause loss of HSP chaperone activity (Muchowski *et al*., 1999).

The *HSP27* gene is located on chromosome 7q11.23 and belongs to the superfamily of small stress induced proteins, and HSP27 protein shows sequence similarity with mammalian α-crystallin proteins (Plumier *et al*., 1997). The expression of *HSP27* is induced in response to various environmental challenges and developmental transitions (Lee *et al*., 2005; Arya *et al*., 2007). As a molecular chaperone, HSP27 protein protects cells from stress, blocks apoptosis signals, and is involved in cell motility and cytoskeletal stabilization (Wagstaff *et al*., 1999; Hirano *et al*., 2004; Heo *et al*., 2006; Williams *et al*., 2006; Arrigo *et al*., 2007). In addition, the overexpression of *HSP27* has been associated with various neurodegenerative diseases, such as Alzheimer's disease (Shimura *et al*., 2004), Parkinson disease (Renkawek *et al*., 1999), Alexander disease (Head *et al*., 1993), and amyotrophic lateral sclerosis (Vleminckx *et al*., 2002).

Magnetic resonance imaging (MRI) is useful for evaluating skeletal muscle physiopathologies (May *et al*., 2000; Farber and Buckwalter, 2002), and thus, in the present study, we tried to identify fatty infiltrations compatible with length-dependent axonal degeneration and sequential muscle involvement in family members.

In this study, we identified a missense mutation, *HSP27* Ser135Phe in 12 members of a large Korean family with dHMN type II, and described the characteristics of clinical and MRI findings of affected members.

Materials and Methods

Subjects

We enrolled 151 unrelated Korean axonal CMT or dHMN families. In the FC197 dHMN family which encompassed six generations, 15 individuals from three generations (IV to VI) were patients, and 12 of these underwent molecular and clinical examinations. Six patients in the upper three generations (I to III) were assumed to have dHMN by history (Figure 1). Paternity and maternity in the FC197 family confirmed by genotyping 15 STR markers using a human identification kit (Applied Biosystems, Foster City, CA). In addition, 200 healthy controls were recruited from our Department of Neurology. All participants included in this study provided written informed consent according to the protocol approved by the Ethics Committee of Ewha Womans University Hospital (Seoul, Korea).

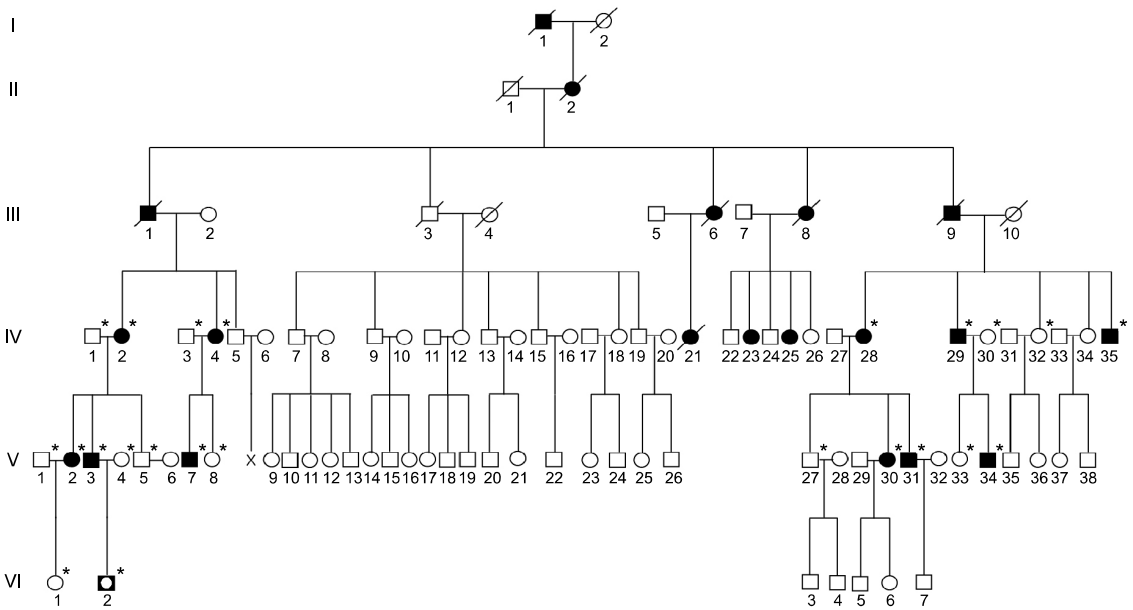

Figure 1. Pedigree of the *HSP27* Ser135Phe mutation in the dHMN family. The open symbols represent unaffected members (□, ○) and filled symbols affected members (■, ●). Half-filled symbol (◘) indicates an unaffected individual harboring the Ser135Phe mutation. Asterisks (*) indicate that a DNA sample was available.

Mutation screening

Genomic DNA was extracted from whole blood using QIAamp DNA blood kits (Qiagen, Hilden, Germany). The 17p11.2-p12 duplication or deletion was first examined for all involved FC197 familial members (affected: 12; unaffected: 11). Then mutations in *HSP27* and in *Cx32, EGR2, MPZ, NEFL, PMP22, MFN2, DNM2, HSP22* and *BSCL2* were screened by direct DNA sequencing of all exons and flanking intronic regions. PCR was carried out in a total volume of 30 μl containing 50 ng of genomic DNA, 0.5 pmol of each primer, 200 μmol of each dNTP, 2 mmol of $MgCl_2$, 0.6 U of *Taq* DNA polymerase and 1X buffer (Promega, Madison, WI), using an GeneAmp PCR system 9700 (Applied Biosystems). PCR consisted of pre-denaturation (94°C for 5 min), 35 amplification cycles (94°C for 40 s, 56°C for 30 s, and 72°C for 90 s), and a final extension (72°C for 7 min). The primer sequences and PCR conditions used are available on request from the corresponding author. PCR products were purified using EXOSAP-IT kits (USB Co.), and analyzed using an ABI 3100 automatic sequencing analyzer (Applied Biosystems). In order to detect sequence variations, we used the SeqScape (Ver. 2.1) program (Applied Biosystems), and confirmed the presence of mutations by analyzing both DNA strands.

Clinical assessment

Clinical information was obtained in a standardized manner, and included assessments of motor and sensory impairments, deep tendon reflexes, and muscle atrophy. Muscle strengths of flexor and extensor muscles were assessed manually using the standard medical research council (MRC) scale. In order to determine physical disability, we used a functional disability scale (FDS) (Birouk *et al*., 1997). Disease severity was determined for each patient using a nine-point FDS, which was based on the following criteria: 0, normal; 1, normal but with cramps and fatigability; 2, an inability to run; 3, walking difficulty but still possible unaided; 4, walking with a cane; 5, walking with crutches; 6, walking with a walker; 7, wheelchair bound; and 8, bedridden. Age at onset was determined by asking patients for their ages when symptoms, i.e., distal muscle weakness, foot deformity, or sensory change, first appeared.

Electrophysiological study

Motor and sensory conduction velocities of median, ulnar, peroneal, tibial, and sural nerves were determined in 12 patients. Recordings were obtained using standard methods with surface stimulation and recording electrodes. Motor conduction velocities (MCVs) of the median and ulnar nerves were determined by stimulating at the elbow or wrist, while recording compound muscle action potentials (CMAPs) over the abductor pollicis brevis and abductor digiti quinti, respectively. In the same way, the MCVs of peroneal and tibial nerves were determined by stimulating at the knee and ankle, while recording CMAPs over the extensor digitorum brevis and abductor hallucis, respectively. CMAP amplitudes were measured from baseline to negative peak values. Sensory conduction velocities (SCVs) were obtained over a finger-wrist segment from the median and ulnar nerves by orthodromic scoring, and were also recorded for sural nerves. Sensory nerve action potential (SNAP) amplitudes were measured from positive peaks to negative peaks.

MRI study

MRI was performed on 12 dHMN patients in a supine position using a 1.5-T system (Siemens Vision; Siemens, Erlangen, Germany). Leg muscle imaging was carried out in axial [field of view (FOV) 24-32 cm, slice thickness 10 mm, and slice gap 0.5-1.0 mm] and coronal planes (FOV 38-40 cm, slice thickness 4-5 mm, slice gap 0.5-1.0 mm). The following protocol was used in all patients: T1-weighted spin-echo (SE) (TR/TE 570-650/14-20, 512 matrixes), T2-weighted SE (TR/TE 2800-4000/96-99, 512 matrixes), and fat-suppressed T2-weighted SE (TR/TE 3090-4900/85-99, 512 matrixes) in both planes. Thigh muscles were explored using the same sequences and planes while adapting field of views and slice thicknesses and gaps. Foot MRI was also studied using the same T1-weighted SE sequence in coronal and axial planes as those detailed above for legs. In addition, a Gd-DTPA (Magnevist, Schering, Germany) contrast enhancement study with fat-suppressed T1-weighted axial SE (TR/TE 600/14, 512 matrixes) was performed in all 12 patients.

Statistical analysis

Differences were evaluated using parametric (Student's *t* test) or non-parametric statistics (Mann-Whitney *U* test), and were considered significant when *P*-values were less than 0.05. All statistical analyses were performed using SPSS for Windows, Ver. 11.0 (SPSS Inc., Chicago, IL).

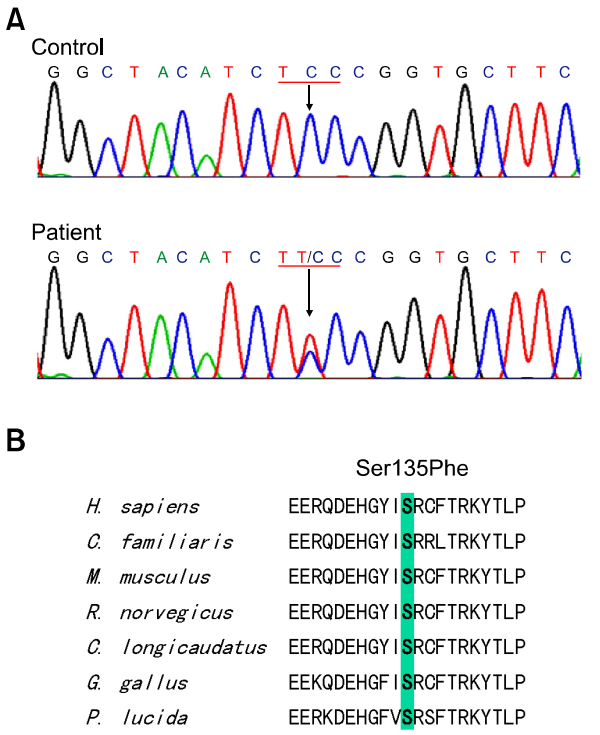

Figure 2. Identification of the *HSP27* Ser135Phe mutation. (A) Sequencing chromatograms showing the C404T (Ser135Phe) mutation in *HSP27* exon 2. Exons were amplified by standard PCR and sequenced using an ABI 3100 automatic sequencer. (B) Conservation of an amino acid at the Ser135Phe mutation site in different species. Multiple alignments of *HSP27* proteins were performed using the ClustalX 1.83 program. The mutation is located on the Hsp20-α-crystallin domain.

Results

Identification of the Ser135Phe mutation in *HSP27*

By mutational screening of the *HSP27* gene in the Korean dHMN family, we identified a heterozygous form of a missense mutation, i.e., c.C404T (Ser135Phe) in exon 2, which has been previously reported to be an underlying cause of CMT2F (Evgrafov *et al*., 2004). In all affected individuals, except VI-2 (who was 4-year-old), the Ser135Phe mutation was found to be well associated with the dHMN phenotype (Figure 1 and 2). This mutation was inherited in an autosomal dominant manner, and was not present in the 200 healthy controls. The mutation site involved is located in the α-crystallin domain, which is highly conserved between species (Figure 2). No 17p11.2-p12 duplication or deletion or causative mutation in the *Cx32, EGR2, MPZ, NEFL, PMP22, MFN2, DNM2, HSP22* or *BSCL2* genes was detected in this family.

Clinical findings

The clinical features of the 12 patients (7 males, 5 females) are shown in Table 1. Muscle weakness and atrophy began and predominated in the distal portions of legs, and were noted to a less extent in distal upper limbs. Paresis in the distal lower limbs varied from asymptomatic to the complete paralysis of distal muscle groups. The ages of the 12 patients ranged from 4 to 62 years (median, 37.5 years), and mean age of onset was 20.6 ± 2.8

Table 1. Clinical findings of dHMN type II patients with the *HSP27* mutation.

Patients	Sex	Age at exam (years)	Age at onset (years)	Disease duration (years)	Muscle weakness[a]				Sensory Loss	Areflexia		FDS[b]	Heel gait defect	Toe gait defect	Hopping defect
					Upper limb		Lower limb			Upper limb	Lower limb				
					Distal	Proximal	Distal	Proximal							
VI-2	M	4	A[c]	0	-	-	-	-	No	No	No	0	No	No	No
V-7	M	25	19	6	-	-	-	-	No	No	No	1	No	No	No
V-34	M	27	18	9	-	-	+	-	No	No	No	1	No	No	No
V-31	M	34	20	14	-	-	+	-	No	No	No	1	No	No	No
V-30	F	36	21	15	-	-	+	-	No	No	No	2	No	No	No
V-3	M	37	17	20	+	-	+	+	No	No	Yes	3	Yes	Yes	Yes
V-2	F	38	18	20	+	-	+	+	No	No	Yes	3	Yes	Yes	Yes
IV-4	F	51	25	26	+	-	++	+	No	No	Yes	3	Yes	Yes	Yes
IV-35	M	51	19	32	+	-	++	+	No	No	Yes	3	Yes	Yes	Yes
IV-29	M	57	24	33	+	-	++	+	No	No	Yes	3	Yes	Yes	Yes
IV-2	F	59	24	35	++	-	++	++	No	Yes	Yes	4	Yes	Yes	Yes
IV-28	F	62	22	40	++	-	++	++	No	Yes	Yes	7	Yes	Yes	Yes

[a]Muscle weakness in lower limbs: + = ankle dorsiflexion 4/5 on medical research council (MRC) scale; ++ = ankle dorsiflexion < 4/5 on MRC scale
Muscle weakness in upper limbs: + = intrinsic hand weakness 4/5 on MRC scale; ++ = intrinsic hand weakness < 4/5 on MRC scale; - = no symptoms;
[b]FDS = functional disability scale, [c]A= asymptomatic.

Table 2. Electrophysiological data of dHMN type II patients with the *HSP27* mutation.

Patients	Age at exam (years)	Motor NCV (m/s)				Sensory NCV (m/s)		
		Median	Ulnar	Peroneal	Tibial	Median	Ulnar	Sural
VI-2	4	56.3 (14.4)	61.7 (11.9)	48.8 (5.4)	51.8 (16.6)	39.5 (26.0)	38.0 (16.9)	37.5 (11.7)
V-7	25	63.8 (18.6)	58.3 (13.4)	43.2 (0.3)	38.7 (0.1)	47.3 (37.4)	41.7 (16.9)	34.3 (26.6)
V-34	26	59.8 (17.4)	59.0 (13.6)	NR	31.2 (0.7)	43.5 (26.7)	40.9 (18.6)	32.8 (13.6)
	27	61.2 (19.5)	60.0 (11.3)	NR	30.1 (0.6)	44.9 (33.8)	41.4 (27.2)	38.1 (13.4)
V-31	33	58.7 (19.4)	50.0 (18.1)	NR	42.0 (0.9)	41.3 (20.5)	40.5 (10.7)	32.4 (12.7)
	34	53.8 (20.1)	52.9 (17.7)	NR	43.8 (1.6)	43.2 (28.5)	40.5 (13.3)	34.4 (23.7)
V-30	35	59.3 (14.6)	55.8 (12.3)	NR	30.8 (0.2)	41.1 (26.6)	38.3 (18.6)	34.7 (10.8)
	36	55.9 (14.8)	55.6 (12.0)	NR	33.5 (0.2)	41.8 (33.5)	38.9 (21.1)	34.3 (13.2)
V-3	36	50.0 (1.4)	51.0 (2.4)	NR	NR	43.2 (15.5)	40.1 (12.4)	37.4 (10.5)
	37	49.1 (1.2)	50.0 (2.1)	NR	NR	42.8 (30.6)	39.9 (12.2)	35.1 (13.1)
V-2	38	38.2 (0.1)	21.8 (0.0)	NR	NR	40.5 (43.9)	40.4 (17.3)	36.2 (14.3)
IV-4	50	50.3 (6.8)	55.0 (7.1)	NR	NR	40.8 (25.7)	39.0 (17.8)	34.3 (24.5)
	51	50.3 (7.5)	53.7 (5.9)	NR	NR	41.1 (32.0)	40.8 (24.9)	33.0 (18.2)
IV-35	50	47.8 (8.1)	42.0 (0.3)	NR	25.2 (0.3)	42.1 (37.6)	37.5 (11.2)	32.2 (27.6)
	51	41.6 (2.1)	41.9 (0.9)	NR	NR	39.6 (23.4)	39.9 (12.5)	33.6 (13.9)
IV-29	57	56.6 (7.0)	47.5 (2.1)	NR	NR	41.2 (28.0)	38.9 (11.9)	32.6 (19.3)
IV-2	58	NR	NR	NR	NR	44.9 (23.1)	39.8 (21.2)	38.3 (17.2)
	59	NR	NR	NR	39.3 (1.4)	44.1 (36.5)	39.1 (23.6)	36.0 (17.8)
IV-28	61	45.8 (8.0)	41.2 (1.1)	NR	NR	41.1 (36.8)	38.7 (9.4)	32.6 (14.4)
	62	46.5 (2.8)	NR	NR	NR	41.6 (32.1)	37.8 (16.7)	34.5 (14.8)

Amplitudes of evoked response are given in parentheses (for motor NCV in mV and for sensory NCV in μV).
Normal NCV values: motor median nerve = ≥ 50.5 m/s; ulnar nerve = ≥ 51.1 m/s; peroneal nerve = ≥ 40.5 m/s; tibial nerve = ≥ 41.1 m/s; sensory median nerve = ≥ 39.3 m/s; ulnar nerve = ≥ 37.5 m/s; sural nerve = ≥ 32.1 m/s.
Normal amplitude values: motor median nerve = ≥ 6 mV; ulnar nerve = ≥ 8 mV; peroneal nerve = ≥ 1.5 mV; tibial nerve = ≥ 6 mV; sensory median nerve = ≥ 8.8 μV; ulnar nerve = ≥ 7.9 μV; sural nerve = ≥ 6.0 μV. NR, not recordable.

years (range, 17-25 years). Mean disease duration was 20.8 ± 12.6 years (range, 0-40 years), and their mean functional disability scale (FDS) score was 2.6 ± 1.8. Interestingly, proximal lower limb and distal upper limb weakness were only observed in patients with disease duration of more than 20 years. No patients showed proximal muscle weakness of upper limbs. Toe gait abnormalities and hopping defect were also observed in patients with long disease duration (≥ 20 years). Sensory loss was absent in all 12 patients.

A sural nerve biopsy examination was carried out at the level of lateral malleolar under local anesthesia in patient V-7. Light microscopy showed a normal myelinated fiber density with a normal fiber diameter distribution, and no evidence of degeneration of single fibers, which was consistent with electrophysiological findings.

Electrophysiological findings

Neurophysiological studies were carried out in the 12 patients (Table 2). Electrophysiological findings confirmed that disease duration was well associated with disease severity. The amplitudes of evoked motor responses were often markedly reduced in those with a long disease duration, and we are unable to record at least one motor nerve in an upper limb in two patients (17%) and in a lower limb in ten patients (83%). All patients, except those with absent NCVs, had at least one motor NCV of > 38 m/s. Sensory nerve conduction velocities and action potentials were noted in all patients.

MRI findings

MRI showed a progression of fatty atrophy with disease duration in thighs and lower legs. Patient V-30 (Figure 3A-C) with 15 years disease duration showed no or only subtle fatty infiltration into thigh muscles, but obvious fatty infiltration or atrophy in the lower leg muscles. In terms of lower leg involvement, the anterolateral muscle compartment was less involved than the other compartment. However, patient IV-28 (Figure 3D-F) with 40 years disease duration showed severe fatty atrophy of the whole lower leg muscle compartments and marked fatty atrophy of thigh muscles with sparing of the gracilis and adductor muscles.

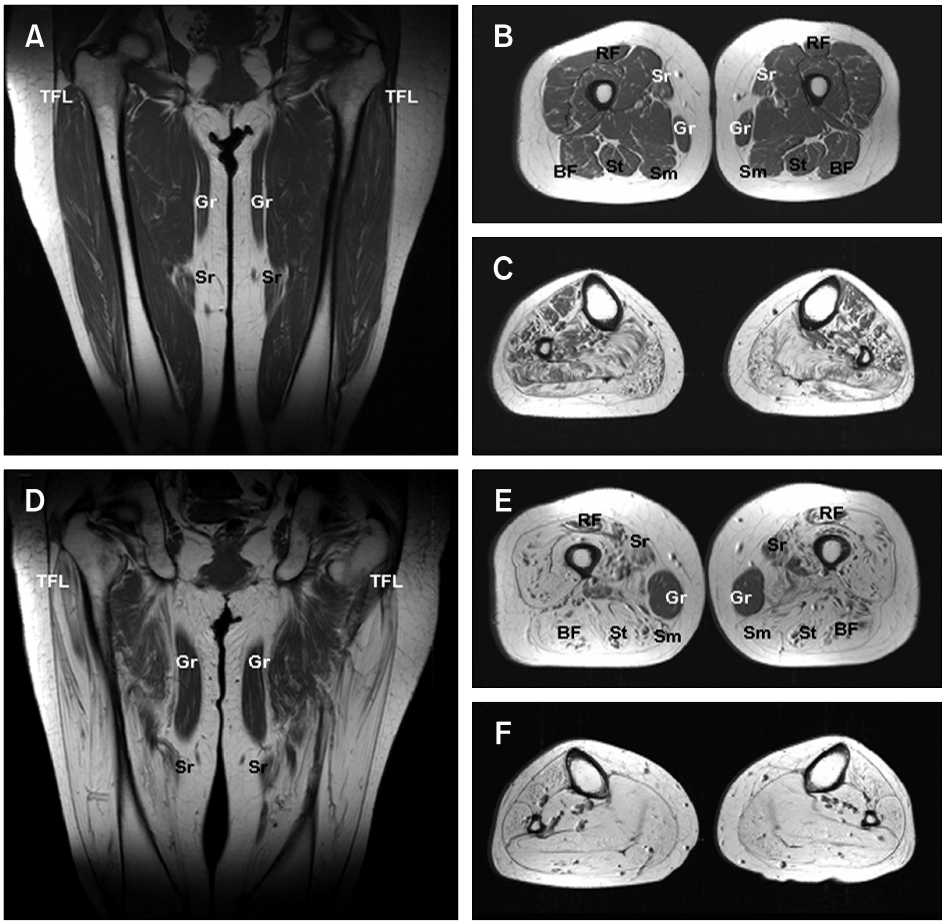

Figure 3. T1-weighted magnetic resonance images (MRI) of the thighs and legs of a patient (V-30) with 15 years disease duration (A-C), and of patient IV-28 with 40 years disease duration (D-F). (A) Anterior coronal thigh image through femoral heads showing subtle fatty infiltration of the vastus muscle group. (B) Middle third axial thigh image showing subtle fatty infiltration of the posterior (BF, biceps femoris; Sm, semimembranosus; and St, semitendinosus) and anterior compartments, but preservation of the sartorius (Sr) and rectus femoris (RF) muscles. Medial compartments are intact. (C) Middle-third axial calf muscle image, showing severe fatty atrophy of the four compartment muscle groups, but a lower degree of anterolateral compartment muscle involvement. (D) Anterior coronal thigh image through femoral heads, showing marked and symmetric hyperintensity, indicative of fatty atrophy of the tensor fasciae latae (TFL) and vastus lateralis muscles, but sparing the gracilis (Gr) and sartorius (Sr) muscles. (E) Middle axial thigh image showing severe fatty atrophy of the posterior compartment and vastus muscle groups of the anterior compartment. Moderate fatty infiltration of the medial compartment and rectus femoris is shown (RF). The preservation of the gracilis (Gr) muscle was noted at this level. (F) Middle third axial calf image showing extensive fatty infiltrations of all four compartments. For comparative purposes the MR images of her daughter with a short disease duration are included (A-C), relatively severe thigh muscle involvements were evident in the mother.

Figure 4 showed progression of fatty atrophy with disease duration in the proximal (A, D, G, J) and mid (B, E, H, K) thigh, and lower leg (C, F, I, L). A male (M/27, Figure 4A-C) and his cousin (M/34, Figure 4D-F) showed very minimal fatty infiltration of posterior compartment of thigh muscle, but mild diffuse involvement of lower leg muscles. However, his uncle (M/51) with 32 years disease duration showed severe fatty atrophy of the posterior and anterior compartments of thigh muscle with less involvement of rectus femoris, sartorius, and adductor longus muscles with sparing of gracilis muscle (Figure 4G-I). Moreover, his aunt (F/59) with 35 years disease duration showed most marked involvement of fatty atrophy in all compartments of thigh muscle with sparing of the gracilis (Figure 4J-L), and her lower legs showed severe fatty atrophy in all muscle compartments.

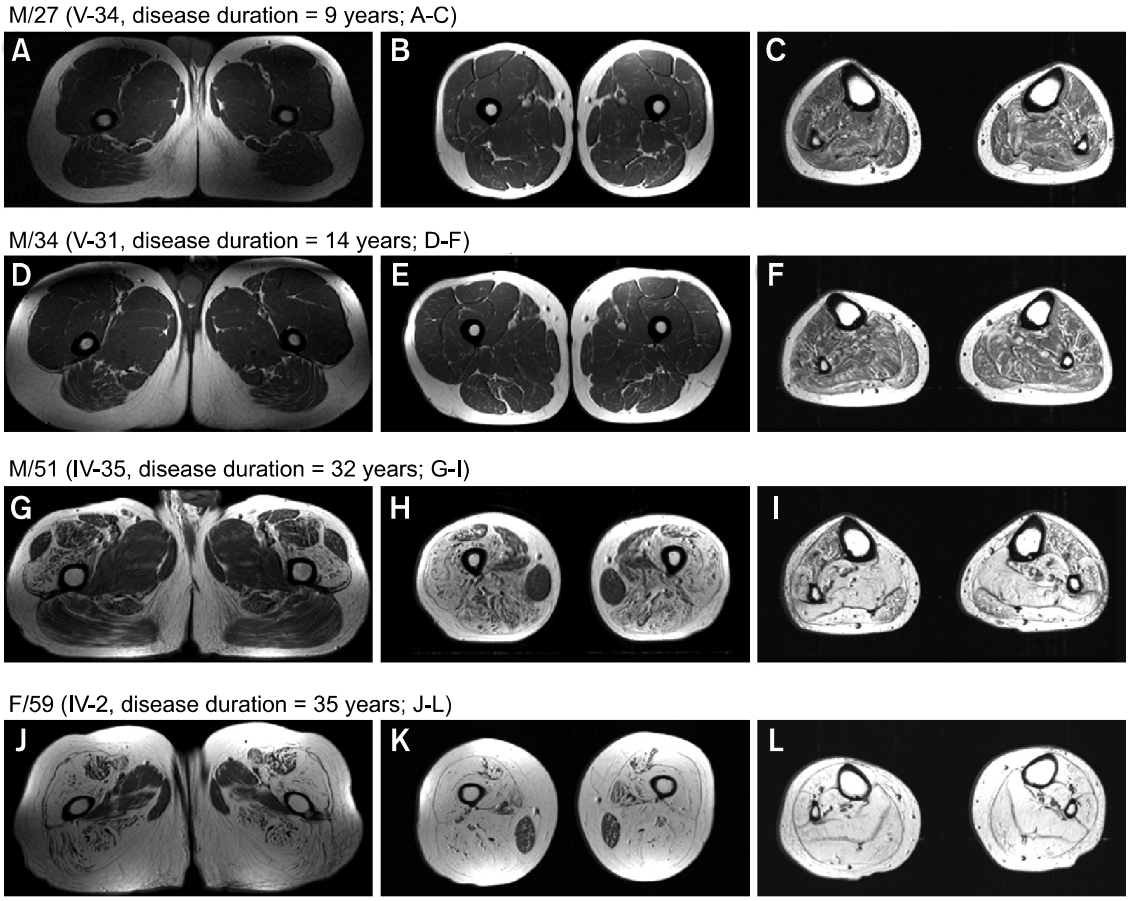

Figure 4. T1-weighted MRI of upper and mid thighs, and legs according to disease progress, i.e., less than 20 years disease duration (A-F) and more than 20 years diseases duration (G-L). Posterior and anterior compartment muscle groups, especially vastus muscles groups, were severely involved in terms of total fatty atrophy, though fatty infiltration in the rectus femoris and sartorius thigh muscles was limited. Gracilis muscle was preserved despite of long disease duration (G-L). In the lower leg, deep and superficial posterior compartments were more severely affected by fatty atrophy than the anterior and extensor digitorum muscle group. However, total fatty atrophy was pronounced in those with a long disease duration, demonstrating the progressive nature of the disease.

Discussion

In this study, we identified a *HSP27* mutation in a large Korean dHMN type II family. The Ser135Phe mutation is located in the highly conserved α-crystallin domain of HSP27 protein, and has been previously reported in two European families, a Russian CMT2 family, and in UK dHMN families (Evgrafov *et al*., 2004). Thus, the Ser135 site in *HSP27* might be a mutational hot spot and an underlying cause of CMT2F and/or dHMN.

The frequency of the *HSP27* mutation was found to be 0.6% among 151 Korean CMT or dHMN families. Evgrafov *et al*. (2004) identified 6 families with *HSP27* mutations after testing 416 European CMT or dHMN unrelated individuals (1.4%). In addition, it has been reported that the frequencies of *HSP27* mutations are 1.4% in the Japanese (Kijima *et al*., 2005), and 0.9% in the Chinese (Tang *et al*., 2005). So, it is believed that *HSP27* gene mutation in patients with CMT or dHMN is not common.

HSP27 has been shown to be essential for the survival of both sensory and motor neurons (Benn *et al*., 2002). The *in vitro* expressions of *HSP27* Ser135Phe mutant protein reduces the viabilities of neuronal cells and impairs neurofilament assembly, which suggests that it is responsible for premature axonal degeneration (Evgrafov *et al*., 2004). In addition, the Ser135Phe or Pro182Leu mutation in *HSP27* was found to result in disruptions of the neurofilament network and of axonal transport in cortical neurons, thus implying that cytoskeletal disruption or neurofilament aggregation has a role in dHMN (Sun and MacRae, 2005; Ackerley *et al*., 2006). One possibility is that molecules of altered

HSP27 may cluster together and interfere with the normal function of nerve cells, particularly axons. In addition, the overexpression of *HSP27* enables injured neonatal motor neurons to reestablish functional contacts with denervated muscle, which results in an improvement in motor unit number, muscle force, and contractile speed (Sharp *et al*., 2006). Recently, it was suggested that the *HSP27* Ser135Phe mutation is associated with increased oligomeric interaction between HSP27 and HSP22 proteins. Moreover, it has been suggested that late onset dHMN may develop from cell damage due to an accumulation of malfunctioning HSP complexes of a protracted period (Fontaine *et al*., 2006).

The *HSP27* Ser135Phe mutation is associated with CMT2F and dHMN, which raises the question as to how this single mutation might lead to various clinical phenotypes. Age at onset in the present family was between 17 and 25 years, and a Russian family with the same mutation had a similar range of onset between the age of 15 and 25 years (Evgrafov *et al*., 2004). However, a Chinese family with the *HSP27* Arg127Trp mutation had a late onset between 35 and 65 years (Tang *et al*., 2005), and a Japanese patient with *HSP27* Pro182Ser developed clinical symptoms at 4 years (Kijima *et al*., 2005). The above findings indicate that individual mutations are associated with specific disease onsets.

In the present study, all affected family members had similar clinical phenotypes and disease progression patterns. The first presenting motor symptom was paresis of extensor muscles of the great toe and later of extensor muscles of the other toes and of the feet. The disease initially paralyses distal muscles of the lower extremities, and progresses to cause muscle weakness and atrophy in the hands and proximal leg muscles. Sensory abnormalities and pyramidal tract signs were absent in all cases, as was pes cavus. In all family members, the disease pursued a slowly progressive course that caused disability of proximal thigh muscles after 20 years of evolution.

Fatty infiltrations in lower limbs by MRI were greater distally, and were thus compatible with the notion of length-dependent axonal degeneration. In IV-28 patients with long disease durations, lower leg fatty infiltrations were so severe that MRI was used to evaluate thighs to observe this length dependency. Thus, our findings are consistent with the hypothesis that length-dependent degeneration of motor axons causes muscle denervation in dHMN patients. These results are useful for differentiating motor neuron disease from peripheral neuropathies like dHMN.

In addition, a tendency was found among this family for fatty infiltrations to progressively extend distal to proximal in lower extremities, and that proximal muscle involvement commenced after a disease duration of 20 years. Fatty atrophy of the thigh progressed to affect the posterior compartment (biceps femoris, semimembranous and semitendinosus muscles) and the anterior compartment, especially the vastus muscle groups, but affected the sartorius and rectus femoris to lesser extents. In the medial compartment, the gracilis muscle was specifically spared even after long disease duration. In terms of comparisons with CMT1A, severe involvements of posterior and medial group muscles have been reported, but with less involvement of anterior compartment muscles, especially the vastus muscle group (Berciano *et al*., 2006). Although dHMN shows similar involvement of posterior compartment muscles, it also severely affects anterior compartment muscles, especially the vastus muscle group, which suggests that the etiologies and pathophysiologies of CMT1A and dHMN differ.

In conclusion, we described the clinical, electrophysiological, and neuroimaging findings of Korean dHMN type II patients. The frequency of *HSP27* mutation was low, and thigh MRI revealed length-dependent degeneration, and different features from that observed in CMT1A patients.

Acknowledgments

This study was supported by the Brain Korea 21 project, Ministry of Education, the Korea Research Foundation Grant funded by the Korean Government (MEST) (KRF-2007-313-E00397), the Agricultural R&D Promotion Center (ARPC-106068- 3) and the RIC/NMR program of MOCIE in Kongju National University.

References

Ackerley S, James PA, Kalli A, French S, Davies KE, Talbot K. A mutation in the small heat-shock protein HSPB1 leading to distal hereditary motor neuronopathy disrupts neurofilament assembly and the axonal transport of specific cellular cargoes. Hum Mol Genet 2006;15:347-54

Arrigo AP, Simon S, Gibert B, Kretz-Remy C, Nivon M, Czekalla A, Guillet D, Moulin M, Diaz-Latoud C, Vicart P. *HSP27* (HspB1) and αB-crystallin (HspB5) as therapeutic targets. FEBS Lett 2007;581:3665-74

Arya R, Mallik M, Lakhotia SC. Heat shock genes-integrating cell survival and death. J Biosci 2007;32:595-610

Benn SC, Perrelet D, Kato AC, Scholz J, Decosterd I, Mannion RJ, Bakowska JC, Woolf CJ. *HSP27* upregulation and phosphorylation is required for injured sensory and motor neuron survival. Neuron 2002;36:45-56

Berciano J, Gallardo E, Garcia A, Infante J, Mateo I, Combarros O. Charcot-Marie-Tooth disease type 1A duplication with severe paresis of the proximal lower limb muscles: a long-term follow-up study. J Neurol Neurosurg Psychiatry 2006;77:1169-76

Birouk N, Gouider R, Le Guern E, Gugenheim M, Tardieu S, Maisonobe T, Le Forestier N, Agid Y, Brice A, Bouche P. Charcot-Marie-Tooth disease type 1A with 17p11.2 duplication. Clinical and electrophysiological phenotype study and factors influencing disease severity in 119 cases. Brain 1997;120:813-23

Evgrafov OV, Mersiyanova I, Irobi J, Van Den Bosch L, Dierick I, Leung CL, Schagina O, Verpoorten N, Van Impe K, Fedotov V, Dadali E, Auer-Grumbach M, Windpassinger C, Wagner K, Mitrovic Z, Hilton-Jones D, Talbot K, Martin JJ, Vasserman N, Tverskaya S, Polyakov A, Liem RK, Gettemans J, Robberecht W, De Jonghe P, Timmerman V. Mutant small heat-shock protein 27 causes axonal Charcot-Marie-Tooth disease and distal hereditary motor neuropathy. Nat Genet 2004;36:602-6

Farber JM, Buckwalter KA. MR imaging in nonneoplastic muscle disorders of the lower extremity. Radiol Clin North Am 2002;40:1013-31

Fontaine JM, Sun X, Hoppe AD, Simon S, Vicart P, Welsh MJ, Benndorf R. Abnormal small heat shock protein interactions involving neuropathy-associated HSP22 (HSPB8) mutants. FASEB J 2006;20:2168-70

Head MW, Corbin E, Goldman JE. Overexpression and abnormal modification of the stress proteins alpha B-crystallin and *HSP27* in Alexander disease. Am J Pathol 1993;143:1743-53

Heo JI, Lee MS, Kim JH, Lee JS, Kim J, Park JB, Lee JY, Han JA, Kim JI. The role of tonicity responsive enhancer sites in the transcriptional regulation of human hsp70-2 in response to hypertonic stress. Exp Mol Med 2006;38:295-301

Hirano S, Shelden EA, Gilmont RR. *HSP27* regulates fibroblast adhesion, motility, and matrix contraction. Cell Stress Chaperones 2004;9:29-37

Irobi J, Dierick I, Jordanova A, Claeys KG, De Jonghe P, Timmerman V. Unraveling the genetics of distal hereditary motor neuronopathies. Neuromolecular Med 2006;8:131-46

Kijima K, Numakura C, Goto T, Takahashi T, Otagiri T, Umetsu K, Hayasaka K. Small heat shock protein 27 mutation in a Japanese patient with distal hereditary motor neuropathy. J Hum Genet 2005;50:473-6

Lee JS, Zhang MH, Yun EK, Geum D, Kim K, Kim TH, Lim YS, Seo JS. Heat shock protein 27 interacts with vimentin and prevents insolubilization of vimentin subunits induced by cadmium. Exp Mol Med 2005;37:427-35

May DA, Disler DG, Jones EA, Balkissoon AA, Manaster BJ. Abnormal signal intensity in skeletal muscle at MR imaging: patterns, pearls, and pitfalls. Radiographics 2000;20:S295-315

Muchowski PJ, Wu GJ, Liang JJ, Adman ET, Clark JI. Site-directed mutations within the core 'alpha-crystallin' domain of the small heat-shock protein, human alphaB-crystallin, decrease molecular chaperone functions. J Mol Biol 1999;289:397-411

Plumier JC, Hopkins DA, Robertson HA, Currie RW. Constitutive expression of the 27-kDa heat shock protein (*HSP27*) in sensory and motor neurons of the rat nervous system. J Comp Neurol 1997;384:409-28

Renkawek K, Stege GJ, Bosman GJ. Dementia, gliosis and expression of the small heat shock proteins *HSP27* and alpha B-crystallin in Parkinson's disease. Neuroreport 1999;10: 2273-6

Sharp P, Krishnan M, Pullar O, Navarrete R, Wells D, de Belleroche J. Heat shock protein 27 rescues motor neurons following nerve injury and preserves muscle function. Exp Neurol 2006;198:511-8

Shimura H, Miura-Shimura Y, Kosik KS. Binding of tau to heat shock protein 27 leads to decreased concentration of hyperphosphorylated tau and enhanced cell survival. J Biol Chem 2004;279:17957-62

Sun Y, MacRae TH. The small heat shock proteins and their role in human disease. FEBS J 2005;272:2613-27

Tang B, Liu X, Zhao G, Luo W, Xia K, Pan Q, Cai F, Hu Z, Zhang C, Chen B, Zhang F, Shen L, Zhang R, Jiang H. Mutation analysis of the small heat shock protein 27 gene in Chinese patients with Charcot-Marie-Tooth disease. Arch Neurol 2005;62:1201-7

Vleminckx V, Van Damme P, Goffin K, Delye H, Van Den Bosch L, Robberecht W. Upregulation of *HSP27* in a transgenic model of ALS. J Neuropathol Exp Neurol 2002;61:968-74

Wagstaff MJ, Collaco-Moraes Y, Smith J, de Belleroche JS, Coffin RS, Latchman DS. Protection of neuronal cells from apoptosis by *HSP27* delivered with a herpes simplex virus-based vector. J Biol Chem 1999;274:5061-9

Williams KL, Rahimtula M, Mearow KM. Heat shock protein 27 is involved in neurite extension and branching of dorsal root ganglion neurons *in vitro*. J Neurosci Res 2006; 84:716-23